Current Research in Environmental Sustainability 4 (2022) 100187

Contents lists available at ScienceDirect

Current Research in Environmental Sustainability

journal homepage: www.sciencedirect.com/journal/current-research-in-environmental-sustainability

# Spatio-temporal variations in the water quality of the Doorndraai Dam, South Africa: An assessment of sustainable water resource management

Mmasabata Dolly Molekoa[a], Pankaj Kumar[b], Bal Krishan Choudhary[c], Ali P. Yunus[d], Ali Kharrazi[e,f], Khaled Mohamed Khedher[g,h], Mohammed J. Alshayeb[m], Bhupendra P. Singh[i], Huynh Vuong Thu Minh[j], Tonni Agustiono Kurniawan[k], Ram Avtar[a,l,*]

[a] Graduate School of Environmental Science, Hokkaido University, Sapporo 060-0810, Japan
[b] Adaptation and Water, Institute for Global Environmental Strategies, Hayama 240-0115, Japan
[c] Department of Environmental Science, Ramthakur College, Agartala, Tripura 799003, India
[d] Department of Environmental Earth Sciences, Indian Institute of Science Education and Research (IISER), Mohali, Punjab, India
[e] Advanced Systems Analysis Group, International Institute for Applied Systems Analysis, Schlossplatz 1, A-2361 Laxenburg, Austria
[f] Global Studies Program, Akita International University, Yuwa City, Akita 010-1292, Japan
[g] Department of Civil Engineering, College of Engineering, King Khalid University, Abha 61421, Saudi Arabia
[h] Department of Civil Engineering, High Institute of Technological Studies, Mrezgua University Campus, Nabeul 8000, Tunisia
[i] Faculty of Environmental Science, Delhi School of Climate Change & Sustainability, Deshbandhu college (Delhi University), New Delhi, India
[j] Department of Water Resources, CENREs, Can Tho University, Can Tho 900000, Viet Nam
[k] Key Laboratory of the Coastal and Wetland Ecosystems, Xiamen University, Xiamen 361102, China
[l] Faculty of Environmental Earth Science, Hokkaido University, Sapporo 060-0810, Japan
[m] Department of Architecture and Planning, College of Engineering, King Khalid University, Abha 61421, Saudi Arabia

ARTICLE INFO

*Keywords:*
Water quality
Remote sensing
Land use land cover
SPM

ABSTRACT

The problem of water scarcity and clean water in sub-Saharan Africa is a growing concern. This study aims to quantify the water quality on a temporal scale in the Doorndraai dam site in sub-Saharan Africa to design possible management options. Here, an integrated approach using both *in-situ* measurements of water quality parameters and remote sensing data was used to derive the water quality index (WQI) and inherent optical properties of water to deduce the factors governing seasonal and annual variability. The results show that all the water quality parameters analyzed fall under the permissible limit of the World Health Organization (WHO) for drinking water, except turbidity. The average value of turbidity for the dry and wet periods was 12.52 and 3.39 NTU, respectively. WQI value ranges from good to excellent during the wet season, and poor in the dry season owing to the high values of turbidity in the water samples. Both *in-situ* and remote sensing-based analysis shows that during the last five years, the value of suspended particulate matter (SPM) based on Landsat-8 increased gradually in the study area. The Sentinel-2 derived modified normalized difference water index (MNDWI) shows a decreasing trend in the water area due to encroachment. The strong correlation between *in-situ* and remote sensing data supports the usefulness of remote sensing techniques for water resource management, especially in data-scarce regions. Looking at the spatio-temporal trend of water quality evolution, the findings of this study will help local decision-makers design sustainable plans for water resource management of Doorndraai dam.

## 1. Introduction

Water is one of the most valuable and finite resources on earth that is significant to the well-being of both humans and ecosystems (Avtar et al., 2011). The key factors that affect this finite resource in terms of both quality and quantity are population growth, land use - changes in land cover, climate change, poor governance, and lack of water treatment infrastructures (Kumar, 2019). Approximately half a billion people across the world live in areas where freshwater consumption exceeds its recharge rate by twofold (Mekonnen and Hoekstra, 2016). Surface water resources are dynamic in nature and prone to both point and non-point sources of pollution. Therefore, regular monitoring of surface water

* Corresponding author at: Graduate School of Environmental Science, Hokkaido University, Sapporo 060-0810, Japan.
*E-mail address:* ram@ees.hokudai.ac.jp (R. Avtar).

https://doi.org/10.1016/j.crsust.2022.100187
Received 13 June 2022; Received in revised form 28 August 2022; Accepted 1 September 2022
Available online 13 September 2022

bodies in terms of its dynamics is necessary for sustainable water resource management and protection of human health and the environment (Kazi et al., 2009; Sila, 2019). The holistic management of water resources for sustainable development is particularly supported by the United Nations, where efforts to maintain access to good quality water continue to be prioritized (Kumar et al., 2021; UN, 2015; UN-HABITAT, 2015).

To achieve holistic water resource management, various approaches and methodological tools have been utilized to elucidate the processes that govern water quality, eg statistical approaches (Avtar et al., 2013; Wang et al., 2017), hydrological simulations for the fate and transport of contaminant (Dutta and Sarma, 2021; Neale et al., 2017), and the development of a water quality index (Taloor et al., 2020). With scientific advancement, spatial technologies like remote sensing and geographical information system (GIS) (Huang et al., 2018; Avtar et al., 2019; Singh et al., 2020; Bhaga et al., 2020), artificial intelligence (Elkiran et al., 2019; Hameed et al., 2017), citizen science (Zheng et al., 2017; Hammou et al., 2017), numerical simulation for scenario-based forecasting (Kumar, 2019; Gorgoglione et al., 2020; Babamiri et al., 2021), and multicriteria analysis (Haider et al., 2015; Cetinkaya and Gunacti, 2018) have also been widely used for monitoring and forecasting water resources in recent years. Among these approaches, remote sensing and GIS is the most widely used, as it has a higher capacity to assess different water quality parameters, *viz.* suspended particulate matters (SPM), chlorophyll-a, and turbidity in near-real time (Yunus et al., 2016, 2020; Avtar et al., 2020). Band ratio approach using satellite data is useful to delineate water covered areas. Recently, MNDWI has been effectively used for enhancing and extracting water covered areas with a background dominated by built-up areas (Xu, 2006). Previous studies explained the role of satellite-based land cover change (LULC) in relation to surface water quality (Shukla et al., 2018). LULC information is important for detecting the extent of human influence on the water environment and management practices (Chowdhury et al., 2020). Hong et al., 2016 investigated that water pollution is positively related to agriculture and urban areas in an inland lake in China. LULC changes induce changes in river water quality and affect various benthic macroinvertebrates in the Mthatha River, South Africa (Niba and Mafereka, 2015). Pullanikkatil et al., 2015 studied the impact of urbanization and agriculture on the water quality of the Likangala River, Malawi, with an increase in anions, cations, and *E. coli* downstream of urban areas. Remote sensing is beneficial to countries with limited resources for designing sustainable water management policies because of multi spatio-temporal data acquisition (Zhang et al., 2002; Liebe et al., 2005; Ogilvie et al., 2016; Ji et al., 2009). For developing countries with data scarcity and limited monitoring stations, it is essential to monitor water resources on a regular basis to achieve global targets such as the Sustainable Development Goals (SDGs) (Elkiran et al., 2019). A well-designed water quality monitoring system can help define water quality problems and their management strategies (Chowdhury et al., 2020).

African countries are at the core of this critical issue, where there are very limited scientific studies, providing excellent evidence for different policy interventions (Kaba et al., 2014; Martinez et al., 2015; Molekoa et al., 2019; Dlamini et al., 2021; Matthews and Bernard, 2015; Bhaga et al., 2020). This study analyzes the surface water quality of the Doorndraai Dam in Limpopo, South Africa. Doorndraai Dam is a dam on Sterk river, Mogalakwena river basin with a catchment area of 595 $km^2$, located in Mokopane with primary purpose is for municipal and industrial use. The Doorndraai dam plays a significant role in the livelihood of around 0.33 million people who live in one of the most agriculturally rich areas of South Africa and are heavily dependent on surface water for their agricultural livelihoods, industrial activities, and daily consumption needs (Molekoa et al., 2021). Despite its high importance, very little is known about the factors responsible for the evolution of water quality and its management strategies for Doorndraai Dam. Therefore, the objective of this study is to assess surface water quality using a synergistic approach of remote sensing and *in-situ* measurements. In addition, a spatio-temporal analysis of water quality was performed considering South African water quality guidelines and statistical modelling. The results of this study could be used to configure the extraction rate for different purposes, and therefore, will be helpful in controlling pollution sources and helping design water quality management in Doorndraai dam for the long term.

## 2. Study area

The Doorndraai Dam is located in the Mogalakwena River catchment area in the Waterberg District, Limpopo province of South Africa with coordinates between 24° 16′45″ S and 28° 46′1″ E (Fig. 1). The dam is located outside of the town of Mokopane and supplies water to the livelihood of approximately 328,905 people (South Africa Statistics, 2016). The climate of the study area is semi-arid with an average annual rainfall of 490 mm (Fig. 2). Most of the rainfall occurs between October and March in the wet season, whereas the dry season spanning between May and September receives very little rainfall. The mokopane weather station data was used in this study, which is closest weather station to the study site. The Doorndraai Dam is a buttress dam that is found on the Sterk River in the Mogalakwena River basin. The reservoir capacity is approximately 46,500,000 $m^3$. The surface area is approximately 560.6 ha and has a catchment of approximately 595 $km^2$. The primary purpose of this dam is to supply water for agriculture, industries, and minor recreational activities such as boat cruises, canoeing, parasailing, and fishing. The dam is operated by South Africa's Department of Water Affairs (DWA). Fig. 1 illustrates the Digital Elevation Model (DEM) and the drainage basin of the Doorndraai Dam. The Shuttle Radar Topographic Mission Digital Elevation Model (SRTM-DEM) data was used to extract the stream order and topography of the study area. This information is useful to analyze the watershed morphometry of the dam drainage area (Radwan et al., 2017). Doorndraai Dam is located on stream order No.3, showing that it is located in the low-elevated areas. Therefore, other streams that flow into the Doorndraai dam have an effect on water quality.

## 3. Materials and methods

The methodology is divided into three parts: a) LULC study, b) hydrochemical analysis based on *in-situ* survey of collected water samples and c) remote sensing-based assessment. The idea behind this integrated approach was to emphasize the importance of spatial tools for analyzing water quality in locations that are either inaccessible or where financial resources are limited for the monitoring of water quality. Fifteen different water quality indicators were used in this investigation, including pH, EC, TDS, turbidity, $Ca^{2+}$, $K^+$, $Mg^{2+}$, $Na^+$, $Cl^-$, $HCO_3^-$, $F^-$, $NH_4{}^+$, Cu and $SO_4^{2-}$ and suspended particle matter. In which the WQI was calculated using 13 different water quality indicators (EC, TDS, turbidity, $Ca^{2+}$, $K^+$, $Mg^{2+}$, $Na^+$, $Cl^-$, $HCO_3^-$, $F^-$, $NH_4^+$, Cu, and $SO_4^2$).

### 3.1. Land cover map of study area

In this study, the South African National Land Cover (NLC) map of 2018 was used, which is freely available from https://www.dffe.gov.za/projectsprogrammes/egis_landcover_datasets. The NCL map was derived from Sentinel-2 data with a spatial resolution of 20 m. The overall precision of the NLC 2018 land cover product is >80%. There were many classes in NLC map therefore, similar classes were grouped into 7 land cover classes based on the objectives of this study. Fig. 3 shows the land cover map based on the NLC map of 2018. Most of the study area is covered with forest, followed by grasslands and commercial agriculture, covering proportions of 57.8%, 17.2% and 10.3% of the total area, respectively (Table 1). Previous studies conducted on land use/land cover change have revealed that agricultural land strongly influences stream nitrogen, phosphorus, and sediments (Arheimer and

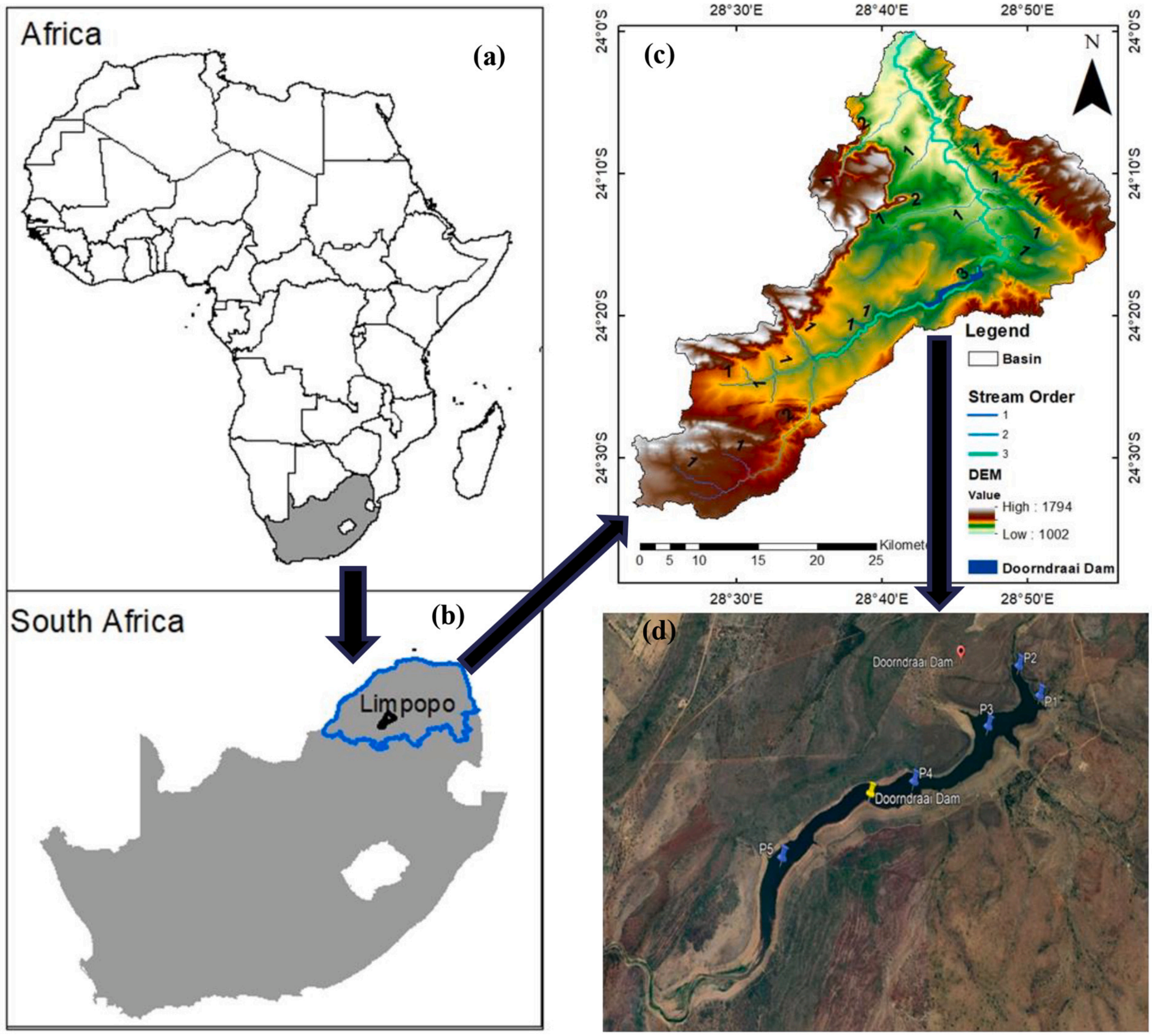


**Fig. 1.** Location of the Doorndraai Dam in Limpopo province of South Africa (a) map of Africa (b) location of South Africa (c) location of the Doorndraai watershed area (d) location of the sampling sites in Doorndraai dam.

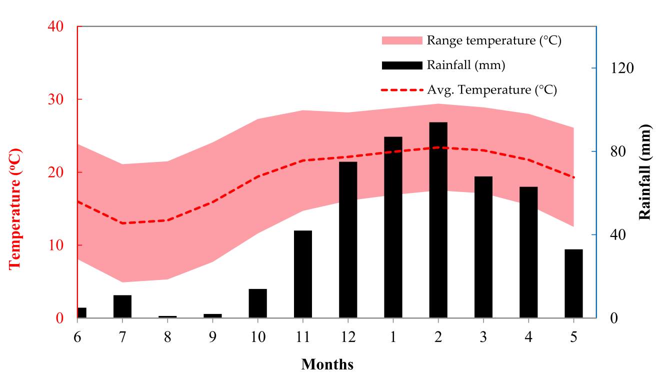


**Fig. 2.** Monthly average rainfall and temperature pattern of study area (Molekoa et al., 2019).

Liden, 2000; Johnson et al., 1997; Smart et al., 1998). Therefore, the use of the LULC map of the study can provide some information on nitrogen, phosphorus, and sediments pollutions in surface water.

### 3.2. *In-situ data collection and laboratory analysis*

Field work was carried out on 6 August 2019 (Dry season) and 25 February (Wet season) in 2020 to collect water samples. Five sampling locations were identified for both seasons using the random sampling technique. Field measurements of pH, EC, TDS, water depth, and temperature were performed using a multiprobe from Orion Model Number 01915. After an *in-situ* analysis, the water samples were filtered with 0.20 μm Millipore filter paper and then collected in pre-rinsed uncontaminated polyethylene bottles. To avoid any fluctuation in the concentration of trace metals, the samples collected for the analysis of the main cations and trace metals were acidified by 1% $HNO_3$ at pH ∼2. The concentration of $HCO_3^-$ was analyzed by acid titration (using Metrohm Multi-Dosimat); while other anions $Cl^-$, $SO_4^{2-}$ and $F^-$ were analyzed by DIONEX ICS-90 ion chromatograph. Inductively coupled plasma-mass spectrometry (ICP-MS) was used to evaluate major cations and trace metals. The relationship between different physio-chemical parameters was performed using a correlation matrix, which also helps in deducing the processes governing water quality (Joshi et al., 2009). In this study, the Pearson's correlation method was used to develop the matrix using SPSS 20.0 software.

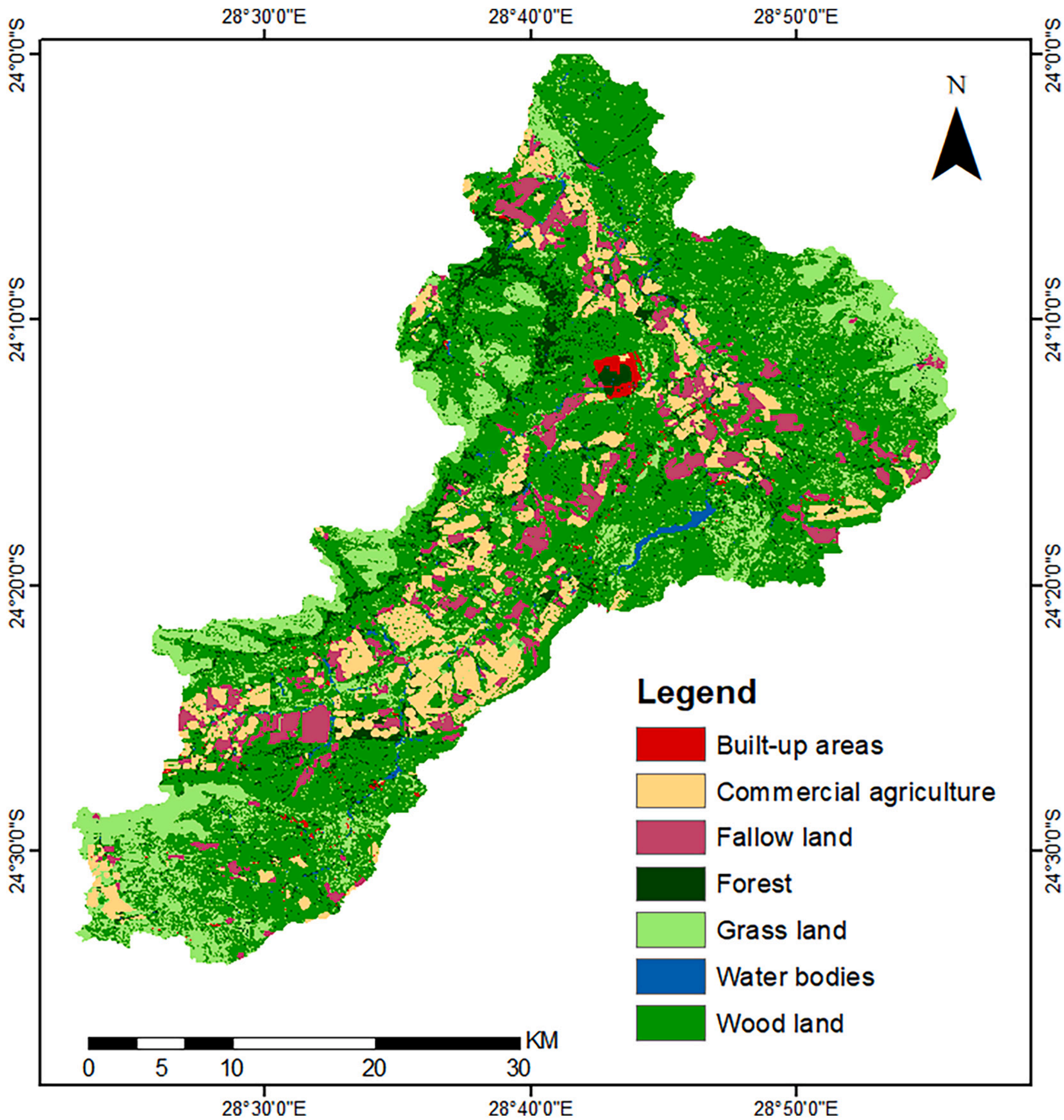


**Fig. 3.** Land cover map of the study area based on NCL-2018 data.

**Table 1**
Land cover classes and area.

| Class name | Area (Km$^2$) | Percentage |
|---|---|---|
| Built-up area | 8.9 | 0.6 |
| Water bodies | 13.3 | 0.9 |
| Forest | 77.6 | 5.3 |
| Fallow land | 114.8 | 7.8 |
| Commercial agriculture | 150.4 | 10.3 |
| Grasslands | 251.6 | 17.2 |
| Woodland | 846.3 | 57.8 |
| Total | 1463.0 | 100.0 |

### 3.3. *Satellite data pre-processing*

The Google Earth Engine (GEE) was used to process satellite data to analyze the surface water quality parameters of Doorndraai Dam. The GEE is an online coding environment that is used to enable relatively rapid server-based analysis responsible for large spatial datasets (Gorelick et al., 2017). The GEE catalogue data comprises observations such as Landsat-8 OLI, Sentinel-2, MODIS (Moderate Resolution Imaging Spectroradiometer), and several climate-gridded datasets, socio-economic, land cover, and geophysical products (Gorelick et al., 2017). In this study, Landsat-8 OLI and Sentinel-2 image collections were used in a GEE environment to analyze suspended particle matter (SPM) and modified normalized difference water index (MNDWI).

#### 3.3.1. *Suspended particle matter (SPM)*

The SPM is defined as the dry mass of particles per unit volume of water (Qiu, 2013). Band 4 (red band) was extracted from Landsat 8 OLI (Operational Land Imager) with 30 m spatial resolution in order to calculate SPM. Previous studies reported the potential of Landsat 8 data to assess temporal variability of SPM (Qiu et al., 2017; Abascal Zorrilla et al., 2018). SPM was calculated for a 5-year period (2015-2020) to monitor temporal variabilities. The following formula of Nechad et al. (2010) was used in order to calculate the SPM from the Landsat-8 surface reflectance products in the GEE environment:

$$SPM = \frac{Apw}{(1 - pw)/C} \tag{1}$$

where, $A$ (289.29) and $C$ (0.1686) are coefficients of empirical models, $pw$ represents the Red Band (B4). The red band empirical algorithm of Nechad et al. (2010) to retrieve the SPM concentrations is well suited for a range of 0–110 mg/L, and therefore is fitted in our studies as well.

#### 3.3.2. Modified normalized difference water index (MNDWI)

Sentinel-2 data with 10 m spatial resolution were used to compute MNDWI using GEE. In this study, MNDWI was used to calculate the water covered area of the Doorndraai dam during the last five-year period (2015-2020). MNDWI can enhance open water features while efficiently suppressing noise from built-up and vegetative areas. Low MNDWI values represented land area, while high values represented water-covered areas. Values below zero were removed as they represented land. The visible green (B3) and short-wavelength infrared 1 (B11) bands of Sentinel-2 data were used to calculate MNDWI (Chen et al., 2015). The infrared 1 (B11) band was resampled to 10 m to calculate MNDWI. The following formula was applied in order to calculate the water boundary of the study area.

$$MNDWI = \frac{B3 - B11}{B3 + B11} \tag{2}$$

### 3.4. Water quality index (WQI) calculation and other statistical analysis

The WQI is one of the most widely used scientific tools for measuring surface water quality around the world (Minh et al., 2019). It provides a single value based on different water quality parameters to compare different samples for quality on the basis of the index value of each sample. The WQI was calculated using 13 different water quality parameters, including EC, TDS, turbidity, $Ca^{2+}$, $K^+$, $Mg^{2+}$, $Na^+$, $Cl^-$, $HCO_3^-$, $F^-$, $NH_4^+$, Cu, and $SO_4^{2-}$. The formula below was used in order to calculate WQI (Molekoa et al., 2019). The following steps were taken to calculate WQI:

A) Calculating the relative weight: It was calculated using Eq. 3.

$$Wi = \frac{wi}{\sum_i^n wi} \tag{3}$$

where $W_i$ represents the relative weight of each parameter sampled, *wi* represents the weight of each parameter, and *n* represents the total number of parameters. All calculated values of $W_i$ are shown in Table 2.

B) Calculating Q value: It was calculated using eq. 4.

$$Qi = \frac{Ci \times 100}{Si} \tag{4}$$

Wherein $Q_i$ = quality rating, $C_i$ = Concentration of each parameter (mg/L), and Si is derived from the WHO water quality standard.

C) Finally, the Water Quality Index (WQI) was calculated using Eq. 5.

$$WQI = \sum Wi \times Qi \tag{5}$$

The WQI was categorized using a method developed by Singh et al. (2011), whereby, WQI < 50 means excellent water quality, WQI = 50–100 means good water quality, WQI = 101–200 means poor water quality, WQI = 200–300 means very poor water quality, and WQI > 300 means unsuitable for drinking. The chemical parameters used for WQI are shown in Table 3.

## 4. Results

### 4.1. General water chemistry

The statistical summary of the water quality analysis is shown in Table 2. It reveals that values/concentrations of all parameters, except turbidity, have fallen within the permissible limit according to South African water quality guidelines (Department of Water Affairs and Forestry, 1996) and WHO guidelines (WHO, 2011) in both dry and wet seasons. Compared to WHO guidelines, the percent of water samples exceeding the turbidity value in dry and wet periods was 100% and 60%, respectively (Table 2). The turbidity value of water bodies is an indicator of high concentration of silt, clays, and other suspended solids, as well as lowered circulation velocity of water. Because of high turbidity not only water looks cloudy but also its aesthetic value decreases a lot (Edokpayi et al., 2015; Nienie et al., 2017). The trend of the average value of the anions were $HCO_3^- > Cl^- > SO_4^{2-} > F^-$, whereas for the cations the trend was $Na^+ > Ca^{2+} > K^+ > Mg^{2+} > NH_4^+$. The main possible source of $Cl^-$ and $SO_4^{2-}$ might be agricultural runoff with an excess of fertilizer input, as shown by the dominance of agricultural

**Table 3**
Relative weights of chemical parameters.

| Parameter | Parameter Standard | qi | Weighted factor | wi | qi x wi |
|---|---|---|---|---|---|
| EC | 150 | 68.73 | 4 | 0.09 | 6.186 |
| TDS | 1000 | 7.34 | 4 | 0.09 | 0.66 |
| Turbidity | 1 | 1558 | 4 | 0.09 | 140.22 |
| $Ca^{2+}$ | 150 | 5.93 | 2 | 0.04 | 0.237 |
| $K^+$ | 15 | 24.33 | 2 | 0.04 | 0.973 |
| $Mg^{2+}$ | 200 | 1.62 | 2 | 0.04 | 0.065 |
| $Na^+$ | 200 | 4.84 | 3 | 0.07 | 0.338 |
| $Cl^-$ | 200 | 4.15 | 4 | 0.09 | 0.374 |
| $HCO_3^-$ | 250 | 5.28 | 4 | 0.09 | 0.475 |
| $F^-$ | 1.5 | 21.33 | 5 | 0.11 | 2.343 |
| $NH_4^+$ | 0.2 | 100 | 5 | 0.11 | 11 |
| Cu | 2 | 0.5 | 5 | 0.11 | 0.055 |
| $SO_4^{2-}$ | 400 | 1.24 | 2 | 0.04 | 0.049 |

**Table 2**
Statistical summary for results from the water quality analysis (Numbers in parentheses show the result for the wet season).

| | Dry season | | | | Wet season | | | | WHO Standard for drinking water (2011) | | |
|---|---|---|---|---|---|---|---|---|---|---|---|
| Parameters | Max | Min | Avg | St Dev | Max | Min | Avg | St Dev | Desire Limit (D. L) | Permissible Limit (P. L) | % of Sample beyond permissible limit |
| pH | 8.30 | 7.20 | 7.60 | 0.60 | 7.90 | 7.10 | 7.40 | 0.45 | 6.50–8.50 | NA | 0 |
| EC (µs/cm) | 173.30 | 158.60 | 165.44 | 5.86 | 140.93 | 123.22 | 133.02 | 7.69 | 500.00 | NA | 0 |
| TDS (mg/L) | 90.10 | 69.50 | 78.00 | 9.68 | 73.00 | 71.00 | 71.80 | 0.84 | NA | NA | NA |
| Turb. (NTU) | 16.50 | 9.34 | 12.52 | 3.27 | 4.25 | 2.31 | 3.39 | 0.94 | 1 | 5.00 | 100 (0) |
| $Ca^{2+}$ (mg/L) | 9.01 | 8.85 | 8.93 | 0.07 | 8.34 | 7.70 | 7.98 | 0.25 | 75.00 | 200.00 | 0 |
| $K^+$ (mg/L) | 4.16 | 3.63 | 3.83 | 0.22 | 3.72 | 3.20 | 3.41 | 0.22 | NA | 200.00 | 0 |
| $Mg^{2+}$ (mg/L) | 3.26 | 3.24 | 3.25 | 0.01 | 3.14 | 2.81 | 2.97 | 0.12 | 50.00 | 150.00 | 0 |
| $Na^+$ (mg/L) | 9.79 | 9.58 | 9.69 | 0.09 | 8.13 | 7.63 | 7.90 | 0.19 | NA | 200.00 | 0 |
| $NH_4^+$ (mg/L) | 0.20 | 0.20 | 0.20 | 0.01 | 0.20 | 0.20 | 0.20 | 0.01 | 0.50 | 0.50 | 0 |
| $F^-$ (mg/L) | 0.32 | 0.30 | 0.32 | 0.01 | 0.26 | 0.24 | 0.25 | 0.01 | 1.00 | 1.50 | 0 |
| $HCO_3^-$ (mg/L) | 44.58 | 36.12 | 40.23 | 3.15 | 27.75 | 16.46 | 21.85 | 5.07 | NA | NA | 0 |
| $Cl^-$ (mg/L) | 8.77 | 8.27 | 8.48 | 0.22 | 6.95 | 6.27 | 6.52 | 0.27 | 200.00 | 600.00 | 0 |
| $SO_4^{2-}$ (mg/L) | 6.52 | 4.94 | 5.58 | 0.66 | 6.64 | 5.69 | 6.18 | 0.45 | 150.00 | 400.00 | 0 |
| Cu (mg/L) | 0.01 | 0.01 | 0.01 | 0.00 | 0.01 | 0.01 | 0.01 | 0.00 | 0.05 | 1.50 | 0 |

**Table 4**
WQI results from *in-situ* measurements.

| | Dry season | | Wet season | |
|---|---|---|---|---|
| Sampling Points | WQI | Water Quality | WQI | Water Quality |
| Site 1 | 166.18 | Poor water | 43.12 | Excellent |
| Site 2 | 111.13 | Poor water | 44.47 | Excellent |
| Site 3 | 122.52 | Poor water | 59.82 | Good water |
| Site 4 | 123.02 | Poor water | 56.82 | Good water |
| Site 5 | 173.93 | Poor water | 58.69 | Good water |

fields in the land use land cover map in Fig. 3.

### 4.2. Water quality index (WQI)

Tables 3 and 4 show the weighting for each of the water quality parameters and their estimated WQI values in both the dry and wet seasons. According to the results, during the dry season, water fell into one category which is 'poor water quality'. The main reason behind this is lowering of stream runoff hence less water availability in the reservoir. During the field work, it was also observed that the dam was only 15% full and the water appeared very milky, indicating high turbidity, which may have resulted from higher evapotranspiration and hence sediment accumulation. The WQI during the wet season fell under excellent and good water categories. This suggests the dilution effect due to rainfall resulting in good water quality.

### 4.3. Correlation matrix

As seen in Table 5, the pH has a strong correlation with $Ca^{2+}$ and $HCO_3^-$ indicating carbonate weathering as the main source of alkalinity of the water resources. The EC variable has a strong positive correlation with turbidity, TDS, $Ca^{2+}$, $Mg^{2+}$, and $HCO_3^-$, whereas moderate association with $Na^+$, $K^+$, $Cl^-$, and $SO_4^{2-}$ indicates the prevalence of carbonate weathering over silicate weathering in addition to anthropogenic inputs like agricultural runoff, improper sewerage management *etc.* Another noticeable association is the positive relation between pH and $F^-$, and negative relations between $Ca^{2+}$ and $F^-$ suggest that the alkaline medium supports the release of fluoride while precipitating calcite and the release of fluoride in the aqueous medium.

### 4.4. Satellite derived SPM

Fig. 5 shows the temporal variation of SPM concentrations in the study site during dry and wet seasons. It can be clearly seen that a definite increase in SPM concentration in the reservoir during the study period, in particular for the years 2019 and 2020 (Fig. 5). Spatial map of SPM also indicates a change in the size of the water covered areas over the years (Fig. 5). Quantitative analysis of SPM showed an increasing trend of SPM concentrations during the past five years for both the dry and wet seasons (Fig. 6). By the end of the observation (*i.e.*, 2020), the SPM concentrations increased about three times from the base period (*i.e.*, 2016) during the dry season, and nearly 4 times during the wet season. The increasing turbidity in the dry periods can be attributed to the decreasing lake coverage area and exposed bottom sediments; whereas the murky water transported by the river, and bottom sediment mixing during the wet season, leading to an increase of SPM. Nevertheless, the SPM values in the dry season is comparatively higher than wet periods (Fig. 6).

### 4.5. The relationship between in-situ and satellite data

The measurement of turbidity determines the level of suspended particle matter, especially of fluvial origin, in water (Wass et al., 1997). The South African water quality standard for turbidity is 1 NTU (Nephelometric Turbidity Unit). *In-situ* measurements show that the turbidity exceeded the permissible limits of South African water quality standards for both dry and wet seasons in our study area (Fig. 4). The dry season (August) in the year 2019 recorded 16.5 NTU as the highest value, whereas the wet season (February) for the year 2020 recorded 4.25 NTU as the highest value.

In the case of satellite data, the Landsat 8 OLI data using the Google Earth Engine was used to calculate SPM for both the dry and wet seasons. In the African region, Kaba et al. (2014) studied the temporal dynamics of an Ethiopian Lake using Landsat data, and Robert et al. (2016) used MODIS data to monitor SPM and turbidity in Bagre reservoir in Burkina Faso. To understand the trend analysis between dry and wet seasons, the SPM was calculated for a five-year time period from 2015 to 2020. The Landsat-8 based SPM results show a good relationship with *in-situ* measured turbidity as they are both influenced by particulate matter in water (Fig. 7). When the SPM increases, the turbidity increases as well, and *vice versa*. Nevertheless, the amounts of SPM did not exactly follow the same pattern as the turbidity values. Although, a linear relation was found between turbidity and SPM concentrations, but that differed between the dry and wet seasons. Similar trend was also noticed

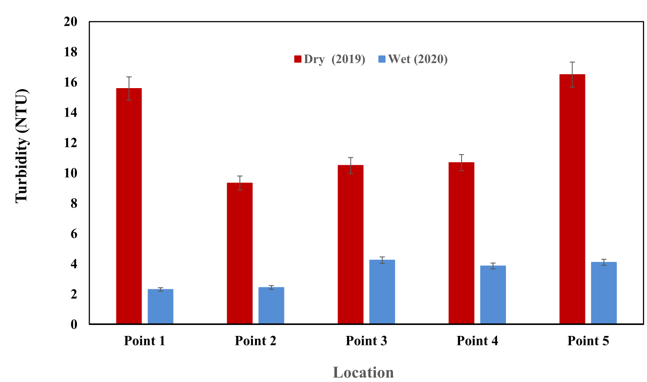


**Fig. 4.** Laboratory analyses for turbidity in dry (August) and wet (February) season.

**Table 5**
Correlation matrix of the water quality parameters.

| | pH | EC | TDS | Turb | $Ca^{2+}$ | $Mg^{2+}$ | $Na^+$ | $K^+$ | $HCO_3^-$ | $Cl^-$ | $SO_4^{2-}$ |
|---|---|---|---|---|---|---|---|---|---|---|---|
| EC | 0.58 | | | | | | | | | | |
| TDS | 0.61 | 0.67 | | | | | | | | | |
| Turb | 0.51 | 0.89 | 0.77 | | | | | | | | |
| $Ca^{2+}$ | 0.59 | 0.82 | 0.53 | 0.61 | | | | | | | |
| $Mg^{2+}$ | 0.50 | 0.71 | 0.56 | 0.58 | 0.89 | | | | | | |
| $Na^+$ | 0.37 | 0.77 | 0.45 | 0.66 | 0.54 | 0.44 | | | | | |
| $K^+$ | 0.32 | 0.78 | 0.38 | 0.29 | 0.22 | 0.15 | 0.75 | | | | |
| $HCO_3^-$ | 0.85 | 0.86 | 0.69 | 0.72 | 0.79 | 0.53 | 0.52 | 0.40 | | | |
| $Cl^-$ | 0.49 | 0.65 | 0.54 | 0.53 | 0.46 | 0.25 | 0.35 | 0.46 | 0.47 | | |
| $SO_4^{2-}$ | 0.44 | 0.54 | 0.27 | 0.38 | 0.39 | 0.31 | 0.52 | 0.22 | 0.54 | 0.42 | |
| $F^-$ | −0.79 | 0.43 | 0.28 | 0.41 | −0.57 | 0.34 | 0.66 | 0.51 | 0.65 | −0.43 | −0.12 |

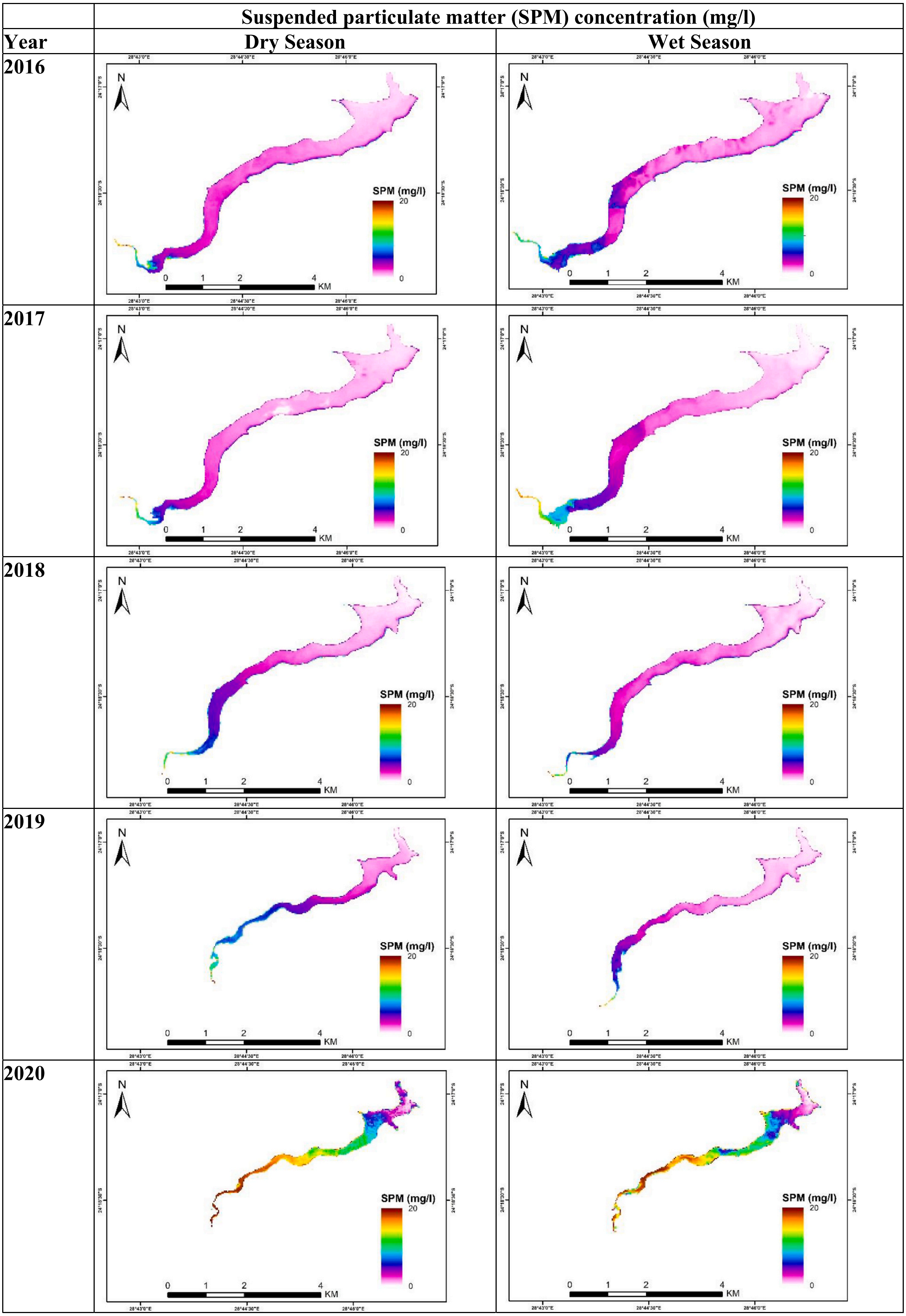


**Fig. 5.** Spatio-temporal variations of SPM concentration estimated for Doorndraai dam in dry and wet season from 2016 to 2020.

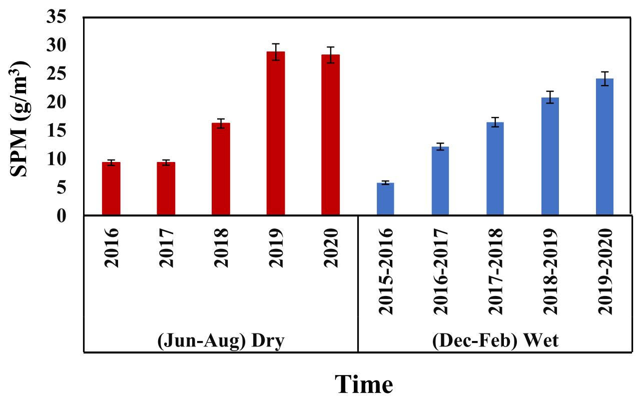


**Fig. 6.** SPM for driest and wettest months in 5 years period.

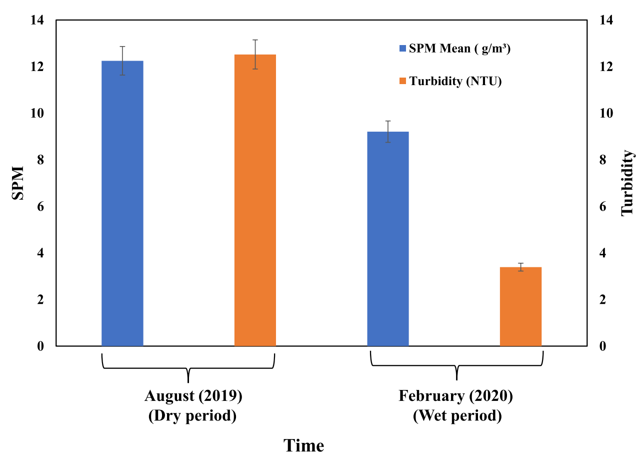


**Fig. 7.** Landsat-8 based mean SPM and *in-situ* mean turbidity in dry and wet season.

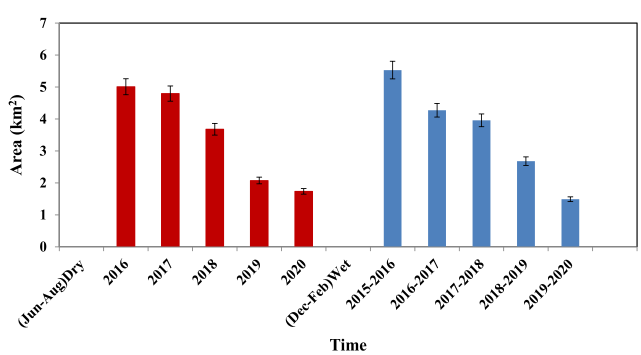


**Fig. 8.** Doorndraai dam water covered area in km$^2$ in 5 years period.

in previous studies as well; for instance, Hellal et al. (2020) reported two distinct linear relationships for the wet and dry seasons between SPM and NTU in Comté-Orapu basin, French Guyana. They attributed this difference to the varying nature of particulate matters during the two seasons. For example, the high turbidity in Doorndraai during dry season is the result of low water level in the lake and associated sediment dynamics, whereas high turbidity in the wet season is the result of a mixed response, *i.e.*, transported murky water and bottom sediment mixing. Results thus support the use of remotely sensed information as an alternative data for long-term analysis.

### 4.6. MNDWI (modified normalized difference water index)

To further examine the impact of changes in the dam area on water quality, the water covered area of Doorndraai Dam was calculated using MNDWI from GEE. Fig. 8 illustrates the temporal changes in the water covered area in the dam. A decreasing trend of water covered area of the Doorndraai Dam is observed in the past five years. For example, year 2016–2017 (both wet and dry season) the highest area of the dam was recorded, whereas, during 2019–2020 the lowest value was recorded. In general, the area for wet seasons is higher than that of dry seasons. The total area was above 5 km$^2$ in the dry season of 2016, which was reduced to below 2 Km$^2$ in the dry period of the year 2020.

## 5. Discussion

The water discharge to the Doorndraai dam is supplied from the Mogalakwena river basin falling in the most densely populated and industrialized catchment in the region. Numerous mines including the AMPLAT Mogalakwena Platinum mine is also located in the catchment (Lombaard et al., 2015). Despite being industrialized, the overall water quality as rated from the WQI except for turbidity is rated good. Nonetheless, the physio-chemical data analyzed from the dam water shows that there were variations during dry and wet seasons. In dry season, the water quality rating changes to poor from being excellent or good as observed during the wet season. Between different sampling sites, the variation in water properties do not change much (see Table 2). One of the major reasons thus for poor WQI in dry period can be attributed to low discharge conditions. The water flow to the dam varies seasonally and very irregular (FAO, 2004). Love et al., 2010 reported that the northern Limpopo basin experiencing a decline in number of rainy days, increases in dry spells, increases in days without flow. The evaporation rate that range between 800 and 2400 mm annually has a mean value of 1970 mm, leading to a higher evaporation rate than the average precipitation (IWMI/ARC, 2003). This leads to particle concentration buildup in the surface of the water. Fig. 9 depicts the annual average rainfall and land surface temperature for the Mogalakwena catchment area; this figure indicates that during the last 10 years, the temperature clearly increased and consequently the evapotranspiration.

Our result is in line with one of the previously published reports by LBPTC (2010), which showed that although water quality in the Limpopo River basin was impacted by several factors like land use change and various development activities, but still water quality was not severe compared to its baseline condition. The water quality in the upper reaches of Limpopo catchment in South Africa is generally good, and TDS ranged from 58 mg/L to 307 mg/L. This study shows that the Landsat-8 derived SPM is related to *in-situ* measured turbidity. Nazirova et al., 2021 also reported a similarly strong correlation between SPM and turbidity in Mzymta river of Russia. Chloride and Sodium dominated in the water quality. Furthermore, the levels of phosphate and nitrate were typically low as represented by average concentrations of <0.05 mg/L and 0.05 mg/L, respectively.

Additionally, during field observation, few small water storage bodies were found around Doorndraai Dam. Since Doorndraai dam is feeding all these small storage systems, it could be one of the reasons behind the declining water covered area of the dam as the water does not reach the dam, especially during the dry season. Factors such as deposition of soil, limited or no vegetation cover and soil erosion around the dam could also have an impact, especially in the dry season as observed during the field survey. Sentinel-2 based MNDWI also shows a decreasing pattern of water covered area in the study site. Other researchers also reported the importance of MNDWI to detect surface water coverage (Ji et al., 2018; Sathianarayanan, 2018; Ali et al., 2019). The physical management of aquifers and rivers as well as wider hydrogeological and hydrological environment of the river basin has an influence on water quality as well as ecological quality. In this way,

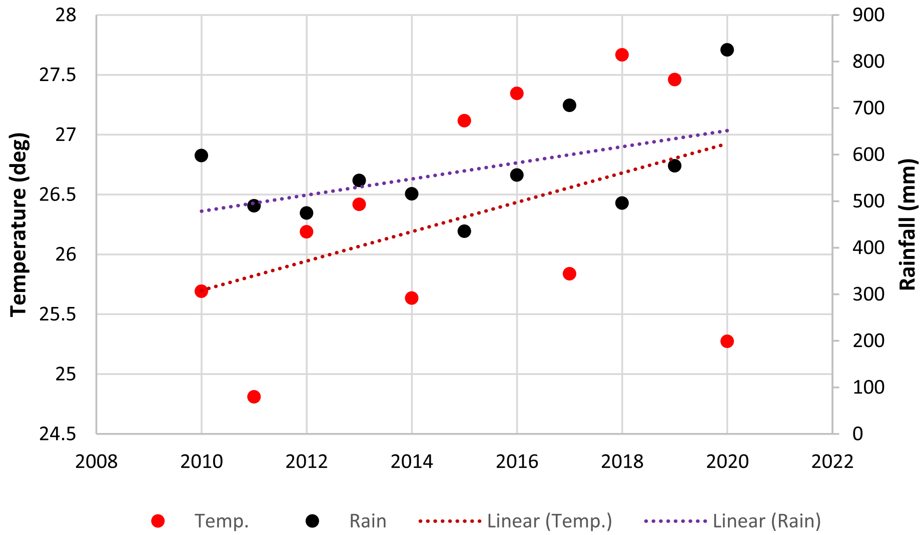


**Fig. 9.** Mean rainfall (CHIRPS) and land surface temperature (MODIS LST) for the study area between 2010 and 2020.

disruptions and changes in natural habitats for example, bank-side vegetation, can be resulted from the physical disturbance from canalization, construction of reservoirs, dredging of rivers, damming as well as other hydrological flow changes such as gravel and sand extraction found in rivers. Such factors have a huge impact on the dam boundary.

Possible new mines are expected to operate in the catchment areas (Lombaard et al., 2015), These new mines add additional water pressure, which could further reduce the water quality, especially in the dry season. It remains to be monitored further whether the pollution still increases in the dam because of additional water stress. Therefore, proper management and close monitoring programs that counter measure the deteriorating problem needs to be initiated as early as possible. Use of multi-temporal *in-situ* data can help us to better understand the relationship between remote sensing and ground based measurement. However, due to limited resources, it was not possible to collect water samples of the study area for a longer period of time.

## 6. Conclusion

This study highlights the temporal analysis of surface water quality using both *in-situ* analysis and remote sensing data in Doorndraai dam, Limpopo, South Africa. The result shows that all the water quality parameters fall under the permissible limit given by the WHO (2011) and South African guidelines (1996) except turbidity. The main reasons behind the excess TDS value are high erosion, evaporation, decay of organic matters *etc.* Study on WQI showed, seasonal changes have significant effects on water quality in both dry and wet season, especially dry season deteriorates the water quality. Looking into the temporal trend of SPM during the last five years period, it shows an increasing trend for turbidity. *In-situ* observation-based turbidity shows a significant correlation with Landsat-8 derived SPM. On the other hand, MNDWI data shows a decreasing trend of water-covered areas for the last five years. The accuracy of remotely sensed data to predict SPM and water coverage area, proved its worth, especially in data-scarce regions. This study shed light on water quality status considering the importance of Doorndraai dam and the absence of any scientific research. This study is vital for designing water management plans and policy toward achieving sustainable water quality as well as SDGs. However, hydrological simulation for future water forecasting should be considered for future study. Moreover, guidelines related to total maximum pollution load and its diligent monitoring at field scale will be necessary to estimate both point and non-point sources of pollutants and guide the policy makers to maintain the ambient water environment healthy. Capacity development is another aspect which needs to be looked after especially for regions completely lacking the skilled manpower required to monitor and manage precious water resources.

## Funding

This research was partially supported by the Deanship of Scientific Research at King Khalid University under the grant number R.G.P. 3/237/43.

## Ethical approval

This research is in compliance with the ethical standard and conduct of the journal.

## Declaration of Competing Interest

The authors declare that they have no known competing financial interests or personal relationships that could have appeared to influence the work reported in this paper.

## Acknowledgement

We would like to acknowledge US Geological Survey (USGS), Sentinel hub, Google Earth and South African National Land (NLC) for providing satellite data and information of the study area. Mmasabata Dolly Molekoa extends gratitude to the JICA-ABE Initiative to provide a scholarship to study master's course at Hokkaido University, Japan. The authors are thankful to the Environmental Department of Ivanplats mine and Albatros Entabeni Camp T/A Honeyguide Ranger Camp for providing assistance during fieldwork and analysis. This work was partially supported by the King Khalid University, Abha, Saudi Arabia (by grant number R.G.P. 3/237/43). We are thankful to anonymous reviewers for their comments.

## References

Abascal Zorrilla, N., Vantrepotte, V., Gensac, E., Huybrechts, N., Gardel, A., 2018. The advantages of Landsat 8-OLI-derived suspended particulate matter maps for monitoring the subtidal extension of Amazonian coastal mud banks (French Guiana). Remote Sens. 10 (11), 1733.

Ali, M.I., Dirawan, G.D., Hasim, A.H., Abidin, M.R., 2019. Detection of changes in surface water bodies urban area with NDWI and MNDWI methods. Int. J. Adv. Sci. Eng. Informat. Technol. 9 (3), 946–951.

Arheimer, B., Liden, R., 2000. Nitrogen and phosphorus concentrations from agricultural catchments—influence of spatial and temporal variables. J. Hydrol. 227 (1–4), 140–159.

Avtar, R., Kumar, P., Singh, C.K., Mukherjee, S., 2011. A comparative study on hydrogeochemistry of ken and Betwa Rivers of Bundelkhand using statistical approach. Water Qual Expo Health 2, 169–179.
Avtar, R., Kumar, P., Surjan, A., Gupta, L.N., Roychowdhury, K., 2013. Geochemical processes regulating groundwater chemistry with special reference to nitrate and fluoride enrichment in Chattarpur area, Madhya Pradesh, India. Environ. Earth Sci. 70, 1699–1708.
Avtar, R., Aggarwal, R., Kharrazi, A., Kumar, P., Kurniawan, A.T., 2019. Utilizing geospatial information to implement SDGs and monitor their progress. Environ. Monit. Assess. 192, 35.
Avtar, R., Kumar, P., Supe, H., Jie, D., Sahu, N., Mishra, B.K., Yunus, A.P., 2020. Did the COVID-19 lockdown-induced hydrological residence time intensify the primary productivity in lakes? Observational results based on satellite remote sensing. Water 12 (9), 2573.
Babamiri, O., Vanaei, A., Guo, X., Wu, P., Richter, A., Ng, K.T.W., 2021. Numerical simulation of water quality and self-purification in a mountainous river using QUAL2KW. J. Environ. Inf. 37 (1), 26–35.
Bhaga, T.D., Dube, T., Shoko, C., 2020. Satellite monitoring of surface water variability in the drought prone Western cape, South Africa. Phys. Chem. Earth, parts A/B/C 102914.
Cetinkaya, C.P., Gunacti, M.C., 2018. Multi-criteria analysis of water allocation scenarios in a water Scarce Basin. Water Resour. Manag. 32, 2867–2884.
Chen, C., Qiming, Q., Li, C., Hong, Z., Abduwasit, Wenzhe F., Chengye, Z., 2015. Photometric correction and reflectance calculation for lunar images from the Chang'E-1 CCD stereo camera. JOSA A 32 (12), 2409–2422.
Chowdhury, M., Hasan, M.E., Abdullah-Al-Mamun, M.M., 2020. Land use/land cover change assessment of Halda watershed using remote sensing and GIS. Egypt. J. Remote Sens. Space Sci. 23 (1), 63–75.
Department of water affairs and forestry, 1996. South African Water Quality Guidelines. In: Aquatic Ecosystem, 7, p. 161. Pretoria, South Africa.
Dlamini, M., Chirima, G., Jovanovic, N., Adam, E., 2021. Assessing the effects of land use on surface water quality in the lower uMfolozi floodplain system, South Africa. Int. J. Environ. Res. Public Health 18, 561.
Dutta, P., Sarma, A.K., 2021. Hydrological modeling as a tool for water resources management of the data-scarce Brahmaputra basin. J. Water Clim. Change 12 (1), 152–165.
Edokpayi, J.N., Odiyo, J.O., Olasoji, S.O., 2015. Assessment of heavy metal contamination of Dzindi River in Limpopo Province, South Africa. Int. J. Nat. Sci. Res. 2, 185–194.
Elkiran, G., Nourani, V., Abba, S.I., 2019. Muliti-step ahead modlleing of river water quality parameters using ensemple artificial intelligence-based approach. J. Hydrol. 577, 123962.
FAO, 2004. Drought impact mitigation and prevention in the Limpopo river basin, A situation analysis. In: Prepared by FAO Subregional Office for Southern and east Africa, Harare. https://www.preventionweb.net/files/1879_VL102146.pdf (accessed on: 13 Jan, 2021).
Gorelick, N., Matt, H., Mike, D., Simon, I., David, T., Rebecca, M., 2017. Google earth engine: planetary-scale geospatial analysis for everyone. Remote Sens. Environ. 202, 18–27.
Gorgoglione, A., Gregorio, J., Alonso, J., Chreties, C., Fossati, M., 2020. Influence of land use/land cover on surface-water quality of Santa Lucía River. Uruguay 12, 4692.
Haider, H., Singh, P., Ali, W., Tesfamariam, S., Sadiq, R., 2015. Sustainability evaluation of surface water quality management options in developing countries: multicriteria analysis using fuzzy UTASTAR method. Water Resour. Manag. 29, 2987–3013.
Hameed, M., Sharqi, S.S., Yaseen, Z.M., Afsan, H.A., Hussain, A., Elshafie, A., 2017. Application of artificial intelligence (AI) techniques in water quality index prediction: a case study in tropical region, Malaysia. Neural Comput. & Applic. 28, 893–905.
Hammou, J.H., Loiselle, S., Ophof, D., Thornhill, I., 2017. Getting the full picture: assessing the complementarity of citizen science and agency monitoring data. PLOS ONE E 12 (12), e0188507.
Hellal, J., Schäfer, J., Vigouroux, R., Lanceleur, L., Laperche, V., 2020. Impact of old and recent gold mining sites on mercury fluxes in suspended particulate matter, water and sediment in French Guiana. Appl. Sci. 10 (21), 7829.
Hong, C., Xiaode, Z., Mengjing, G., Wei, W., 2016. Land use change and its effects on water quality in typical inland lake of arid area in China. J. Environ. Biol. 37, 603–609.
Huang, C., Chen, Y., Zhang, S., Wu, J., 2018. Detecting, extracting, and monitoring surface water from space using optical sensors: a review. Rev. Geophys. 56, 333–360. https://doi.org/10.1029/2018RG000598.
IWMI/ARC, 2003. Limpopo basin profile. In: CGIAR Challenge Program on Water and Food. Pretoria, South Africa, p. 132.
Ji, L., Zhang, L., Wylie, B., 2009. Analysis of dynamic thresholds for the normalized difference water index. Photogramm. Eng. Remote. Sens. 75 (11), 1307–1317.
Ji, X., Li, Y., Luo, X., He, D., 2018. Changes in the lake area of tonle sap: possible linkage to runoff alterations in the lancang river? Remote Sens. 10 (6), 866.
Johnson, L., Carl, R., George, H., John, A., 1997. Landscape influences on water chemistry in Midwestern stream ecosystems. Freshw. Biol. 37 (1), 193–208.
Joshi, D.M., Bhandari, N.S., Kumar, A., Agrawal, N., 2009. Statistical analysis of physicochemical parameters of water of river ganga in Haridwar District. Rasayan J. Chem. 2 (3), 579–587.
Kaba, E., Philpot, W., Steenhuis, T., 2014. Evaluating suitability of MODIS-Terra images for reproducing historic sediment concentrations in water bodies: Lake Tana, Ethiopia. Int. J. Appl. Earth Obs. Geoinf. 26, 286–297.
Kazi, T., Arain, M., Jamali, M.K., Jalbani, N., Afridi, H., Sarfraz, R., Baig, J., Shah, A.Q., 2009. Assessment of water quality of polluted Lake using multivariate statistical techniques: a case study. Ecotoxicol. Environ. Saf. 72, 301–309.
Kumar, P., 2019. Numerical quantification of current status quo and future prediction of water quality in eight Asian mega cities: challenges and opportunities for sustainable water management. Environ. Monit. Assess. 191, 319. https://doi.org/10.1007/s10661-019-7497-x.
Kumar, P., Dasgupta, R., Dhyani, S., Kadaverugu, R., Johnson, B.A., Hashimoto, S., Sahu, N., Avtar, R., Saito, O., Chakraborty, S., Mishra, B.K., 2021. Scenario based hydrological modeling for designing more climate resilient water resource management measures: a case of Brahmani river, Odisha, Eastern India. Sustainability 13, 6339.
LBPTC [Limpopo Basin Permanent Technical Committee], 2010. Joint Limpopo River Basin study, Scoping report. LBPTC, Maputo, p. 91. http://www.limcom.org/_system/writable/DMSStorage/1031en/LIMCOM2010_ScopingStudy_Eng.pdf (Accessed 20 May 2020).
Liebe, J.N., Giesen, V.D., Andreini, M., 2005. Estimation of small reservoir storage capacities in a semi-arid environment: a case study in the upper east region of Ghana. Phys. Chem. Earth, Parts A/B/C 30 (6–7), 448–454.
Lombaard, J., Pieterse, H.S., Rossouw, J.R., Nditwani, T., 2015. Project Name: Limpopo Water Management Area North Reconciliation Strategy.
Love, D., Uhlenbrook, S., Twomlow, S., Van der Zaag, P., 2010. Changing hydroclimatic and discharge patterns in the northern Limpopo Basin, Zimbabwe. SA J. Radiol. 36 (3).
Martinez, J.M., Espinoza-Villar, R., Armijos, E., Moreira, L.S., 2015. The optical properties of river and floodplain waters in the Amazon River basin: implications for satellite-based measurements of suspended particulate matter. J. Geophys. Res. Earth Surf. 120 (7), 1274–1287.
Matthews, M.W., Bernard, S., 2015. Eutrophication and cyanobacteria in South Africa's standing water bodies: a view from space. S. Afr. J. Sci. 111 (5/6).
Mekonnen, M.M., Hoekstra, A.Y., 2016. Four billion people facing severe water scarcity. Sci. Adv. 2 (2), e1500323.
Molekoa, M.D., Avtar, R., Kumar, P., Minh, H.V.T., Kurniawan, A.T., 2019. Hydrochemical assessment of groundwater quality of Mokopane area, Limpopo South Africa using statistical approach. Water 11, 1891. https://doi.org/10.3390/w11091891.
Minh, H.V.T., Avtar, R., Kumar, P., Tran, D.Q., Ty, T.V., Behera, H.C., Kurasaki, M., 2019. Groundwater quality assessment using fuzzy-AHP in An Giang Province of Vietnam. Geosciences 9 (330), 1–23. https://doi.org/10.3390/geosciences9080330.
Molekoa, M.D., Avtar, R., Kumar, P., Minh, T.H.V., Dasgupta, R., Johnson, B.A., Sahu, N., Verma, R.L., Yunus, A.P., 2021. Spatio-temporal analysis of surface water quality in Mokopane area, Limpopo, South Africa. Water 13, 220.
Nazirova, K., Alferyeva, Y., Lavrova, O., Shur, Y., Soloviev, D., Bocharova, T., Strochkov, A., 2021. Comparison of in situ and remote-sensing methods to determine turbidity and concentration of suspended matter in the estuary zone of the mzymta river, black sea. Remote Sens. 13 (1), 143.
Neale, P.A., Altenburger, R., Aissa, S.A., Brion, F., Busch, W., Umbuzeiro, G.A., Denison, M.S., Pasquier, D.D., Hilscherova, K., Hollert, H., Morales, D.A., Novak, J., Schlichting, R., Sieler, T.B., Serra, H., Shao, Y., Tindall, A.J., Tollefsen, K.E., Williams, T.D., Escher, B.I., 2017. Development of a bioanalytical test battery for water quality monitoring: fingerprinting identified micropollutants and their contribution to effects in surface water. Water Res. 123, 734–750.
Nechad, B., Ruddick, K.G., Park, Y., 2010. Calibration and validation of a generic multisensor algorithm for mapping of Total suspended matter in turbid waters. Remote Sens. Environ. 114 (4), 854–866.
Niba, A.S., Mafereka, S.P., 2015. Benthic macroinvertebrate assemblage composition and distribution pattern in the upper Mthatha River, eastern cape, South Africa. Afr. J. Aquat. Sci. 40, 133–142.
Nienie, A.B., Sivalingam, P., Laffite, A., Ngelinkoto, P., Otamonga, J.P., Matand, A., Mulaji, C.K., Mubedi, J.I., Mpiana, P.T., Pote, J., 2017. Seasonal variability of water qulaity by physicochemical indexes and traceable metals in suburban area in Kikwit, Democratic Republic of the Congo. Int. Soil Water Conservat. Res. 5, 158–165.
Ogilvie, A., Belaud, G., Massuel, S., Mulligan, M., Goulven, P.L., Calvez, R., 2016. Assessing floods and droughts in ungauged small reservoirs with Long-term Landsat imagery. Geosciences 6 (4), 42.
Pullanikkatil, D., Palamuleni, L.G., Ruhiiga, T.M., 2015. Impact of land use on water quality in the Likangala catchment, southern Malawi. Afr. J. Aquat. Sci. 40, 277–286.
Qiu, Z., 2013. A simple optical model to estimate suspended particulate matter in Yellow River estuary. Opt. Express 21 (23), 27891–27904.
Qiu, Z., Xiao, C., Perrie, W., Sun, D., Wang, S., Shen, H., He, Y., 2017. Using L andsat 8 data to estimate suspended particulate matter in the Y ellow R iver estuary. J. Geophys. Res. Oceans 122 (1), 276–290.
Radwan, F., Alazba, A.A., Mossad, A., 2017. Watershed morphometric analysis of Wadi Baish dam catchment area using integrated GIS-based approach. Arab. J. Geosci. 10 (12), 1–11.
Robert, E., Grippa, M., Kergoat, L., Pinet, S., Gal, L., Cochonneau, G., Martinez, J.M., 2016. Monitoring water turbidity and surface suspended sediment concentration of the Bagre reservoir (Burkina Faso) using MODIS and field reflectance data. Int. J. Appl. Earth Obs. Geoinf. 52, 243–251.
Sathianarayanan, M., 2018. Assessment of surface water dynamics using multiple water indices around Adama Woreda, Ethiopia. In: ISPRS Annals of the Photogrammetry, Remote Sensing and Spatial Information Sciences, 4, pp. 181–188.
Shukla, A.K., Pathak, S., Pal, L., Ojha, C.S.P., Mijic, A., Garg, R.D., 2018. Spatio-temporal assessment of annual water balance models for upper ganga basin. Hydrol. Earth Syst. Sci. 22, 5357–5371.

Sila, O.N., 2019. Physico-chemical and bacteriological quality of water sources in rural settings, a case study of Kenya, Africa. Sci. Afr 2, E00018.
Singh, C.K., Shashtri, S., Mukherjee, S., Kumari, R., Avatar, R., Singh, A., Singh, R.P., 2011. Application of GWQI to assess effect of land use change on groundwater quality in lower Shiwaliks of Punjab: remote sensing and GIS based approach. Water Resour. Manag. 25 (7), 1881–1898.
Singh, S., Bhardwaj, A., Verma, V.K., 2020. Remote sensing and GIS based analysis of temporal land use/land cover and water quality changes in Harike wetland ecosystem, Punjab, India. J. Environ. Manag. 262, 110355.
Smart, R.P., Soulsby, C., Neal, C., Wade, A., Cresser, M.S., Billett, M.F., Langan, S.J., Edwards, A.C., Jarvie, H.P., Owen, R., 1998. Factors regulating the spatial and temporal distribution of solute concentrations in a Major River system in NE Scotland. Sci. Total Environ. 221 (2–3), 93–110.
Statistics South Africa, 2016. n.d. http://www.statssa.gov.za/.
Taloor, A.K., Pir, R.A., Adimalla, N., Ali, S., Manhas, D.S., Roy, S., Singh, A.K., 2020. Spring water quality and discharge assessment in the Basantar watershed of Jammu Himalaya using geographic information system (GIS) and water quality index (WQI). Groundw. Sustain. Dev. 10, 100364.
UN, 2015. Transforming our World: The 2030 Agenda for Sustainable Development. New York: United Nation. http://www.un.org/ga/search/view_doc.asp?symbol=A/RES/70/1&Lang=E.
United Nations Human Settlements Program (UN-HABITAT), 2015. The United Nations Economic and Social Commission for Asia and the Pacific (UN-ESCAP), The State of Asian and Pacific Cities 2015, Urban Transformations Shifting from Quantity to Quality. ISBN: (Volume) 978–92–1-132681-9.
Wang, J., Liu, G., Liu, H., Lam, P.K.S., 2017. Multivariate statistical evaluation of dissolved trace elements and a water quality assessment in the middle reaches of Huaihe River, Anhui, China. Sci. Total Environ. 583, 421–431.
Wass, P.D., Marks, S.D., Finch, J.W., Leeks, G.J.L., Ingram, J.K., 1997. Monitoring and preliminary interpretation of in-river turbidity and remote sensed imagery for suspended sediment transport studies in the Humber catchment. Sci. Total Environ. 194, 263–283.
World Health Organization (WHO), 2011. Guidelines or Drinkingwater Quality, 4th edn, p. 563. Geneva.
Xu, H., 2006. Modification of normalised difference water index (NDWI) to enhance open water features in remotely sensed imagery. Int. J. Remote Sens. 27 (14), 3025–3033.
Yunus, A.P., Dou, J., Sravanthi, N., 2016. Remote sensing of chlorophyll-a as a measure of red tide in Tokyo Bay using hotspot analysis. Rem. Sens. Applicat. Soc. Environ. 2, 11–25.
Yunus, A.P., Masago, Y., Hijioka, Y., 2020. COVID-19 and surface water quality: improved lake water quality during the lockdown. Sci. Total Environ. 731, 139012.
Zhang, Y., Pulliainen, J., Koponen, S., Hallikainen, M., 2002. Application of an empirical neural network to surface water quality estimation in the Gulf of Finland using combined optical data and microwave data. Remote Sens. Environ. 81 (2–3), 327–336.
Zheng, H., Hong, Y., Long, D., Jing, H., 2017. Monitoring surface water quality using social media in the context of citizen science. Hydrol. Earth Syst. Sci. 21, 949–961.